

Advanced Propulsion Integrated within Structure

a project presented to
The Faculty of the Department of Aerospace Engineering
San José State University

in partial fulfillment of the requirements for the degree
Master of Science in Aerospace Engineering

by

Jack R. Gallagher

December 2022

approved by

Dr. Papadopoulos
Faculty Advisor



San José State
UNIVERSITY

© 2022
Jack R. Gallagher
ALL RIGHTS RESERVED

ABSTRACT
Advanced Propulsion Integrated within Structure

Jack R. Gallagher

The purpose of this paper is to take the propulsion system of a CubeSat and integrate it into the structure. This CubeSat will be additively manufactured and will utilize cold gas as the propellant. The structure and propulsion systems will have to be modeled into CAD software where the pathing for the propellant will have to connect the tank to the individual thrusters. The analysis will then be completed on the structure and propulsion systems to determine the capabilities of this design.

Table of Contents

Abstract	iii
List of Tables	v
List of Figures	vi
List of Symbols	vii
1. Introduction	1
1.1 Motivation	1
1.2 Literature Review	1
1.3 Project Proposal	8
1.4 Methodology	8
2. CubeSat Design	9
2.1 Structure	9
2.2 Skeletal Structure	10
2.3 Propulsion	11
3. CubeSat Launcher	14
3.1 CubeSat Launcher	14
4. Communication	16
4.1 Antenna	16
5. Power System	18
5.1 Battery	18
5.2 Solar Panels	18
6. Analysis	20
6.1 Finite Element Analysis	20
6.2 Thrust Analysis	26
7. Conclusion	29
References	30
Appendix A	33

List of Tables

Table 6.1 - Nozzle and throat data.....	28
Table 6.2 - Equation results.....	28

List of Figures

Figure 1.1 - CubeSat arrangements.....	1
Figure 1.2 - Binder jetting.....	2
Figure 1.3 - Directed energy deposition.....	3
Figure 1.4 - Material extrusion.....	4
Figure 1.5 - Material jetting	5
Figure 1.6 - Powder bed fusion.....	5
Figure 1.7 - Sheet lamination.....	6
Figure 1.8 - Vat photopolymerization.....	7
Figure 2.1 - First iteration of APIS.....	9
Figure 2.2 – Second iteration of APIS.....	10
Figure 2.3 – Piping for the propulsion system.....	12
Figure 2.3 – Zoom in on piping.....	13
Figure 3.1 – Dimensions for CubeSat launcher.....	14
Figure 3.2 – CubeSat General Testing Flow Diagram.....	15
Figure 4.1 – Layout of four wire antennas.....	16
Figure 4.2 – Tape spring rolled up.....	17
Figure 5.1 – Panels with solar panels.....	19
Figure 6.1 - Load Factors for Falcon 9 rocket.....	20
Figure 6.2 – Displacement for the first pair.....	21
Figure 6.3 - Displacement for the second pair.....	22
Figure 6.4 - Safety Factor for the first pair.....	23
Figure 6.5 - Safety Factor for the second pair.....	24
Figure 6.6 - Von Mises Stress for the first pair.....	25
Figure 6.7 - Von Mises Stress for the second pair.....	26

List of Symbols

Symbol	Definition	Units (SI)
F	Force	N
m	Mass	kg
a	Acceleration	m/s^2
F_T	Thrust Force	N
\dot{m}	Mass Flow Rate	kg/s
V_e	Exit Velocity	m/s
P_e	Exit Pressure	Pa
P_a	Ambient Pressure	Pa
A_e	Exit Area	m
A^*	Inlet Area	m
T_e	Chamber Temperature	K
T_t	Inlet Temperature	K
γ	Specific Heat Ratio	
R	Gas Constant	

1. Introduction

1.1 Motivation

CubeSats are the current focus for space programs located at the edge of Earth's atmosphere or just beyond it. These miniature satellites reduce the funds necessary for organizations to place them into orbit and this makes space experiments more accessible. The cost of the launch is almost nonexistent since CubeSats can be taken to space on rockets that are already planned to launch into space [1]. Improvements to the design of these satellites are inevitable in the future since the low cost allows for multiple design iterations and testing. The current precedent for CubeSats is to have a structure designed solely to encase and protect all the inner components.

1.2 Literature Review

CubeSats are a class of small satellites that have a standard size of one unit called 1U. This is measured to be 10cm x 10cm x 10cm [2]. The size can be changed to different sizes with the most common being 1U, 2U, 3U, and 6U as shown in Figure 1.1. This relatively small size allows for them to accompany spacecraft with preplanned launches as cargo. These satellites are mainly placed into low Earth orbit to complete experiments that would be unreasonable to complete on larger satellites due mainly to the resulting cost.

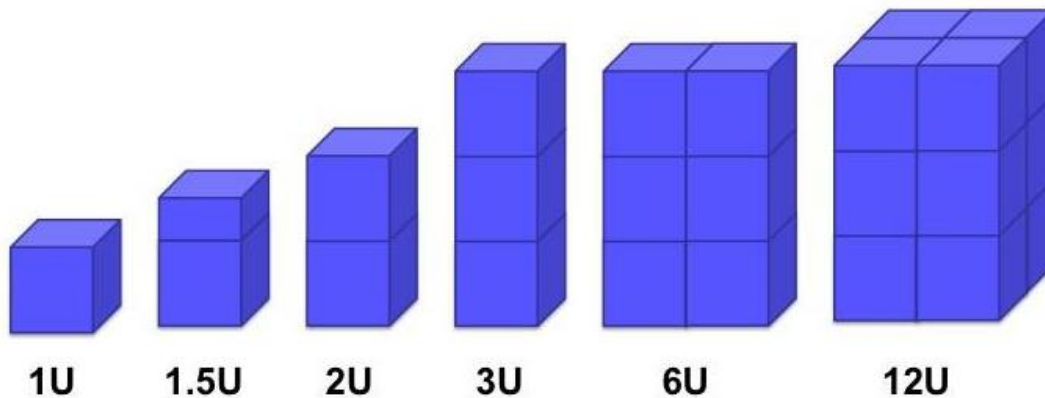


Figure 1.1 – CubeSat arrangements [3].

Additive Manufacturing (AM) is the process where a model is designed within a computer-aided design (CAD) program and then through the different processes is manufactured into three dimensions. This is completed by the model being digitally sliced into thin layers and then printed by those thin layers into a three-dimensional part of the model. This process has decreased the manufacturing time, weight, prototyping time, and capital for the production process. AM allows for parts to be designed and created that otherwise would be impossible from subtractive manufacturing processes. This process is relatively new and has been continuously applied to different aspects of engineering fields.

In an article titled “Additive manufacturing: scientific and technological challenges, market uptake and opportunities” written by Syed Tofail and associates, they state that according to the International Organization for Standardization (ISO) and American Society for Testing and

Materials (ASTM), AM should be separated into seven different sections. These seven processes are binder jetting (BJ), directed energy deposition (DED), material extrusion (ME), material jetting (MJ), powder bed fusion (PBF), sheet lamination (SL), and vat photopolymerization (VP) [4].

BJ has a thin liquid binder that is released onto thin layers of powder that joins the material together [5]. This material created with this process is not suitable to be utilized in structural situations since the powder is bonded together with an adhesive. The mechanical layout for BJ is shown in Figure 1.2. This process is relatively quick and can be created using materials such as metals, polymers, or ceramics.

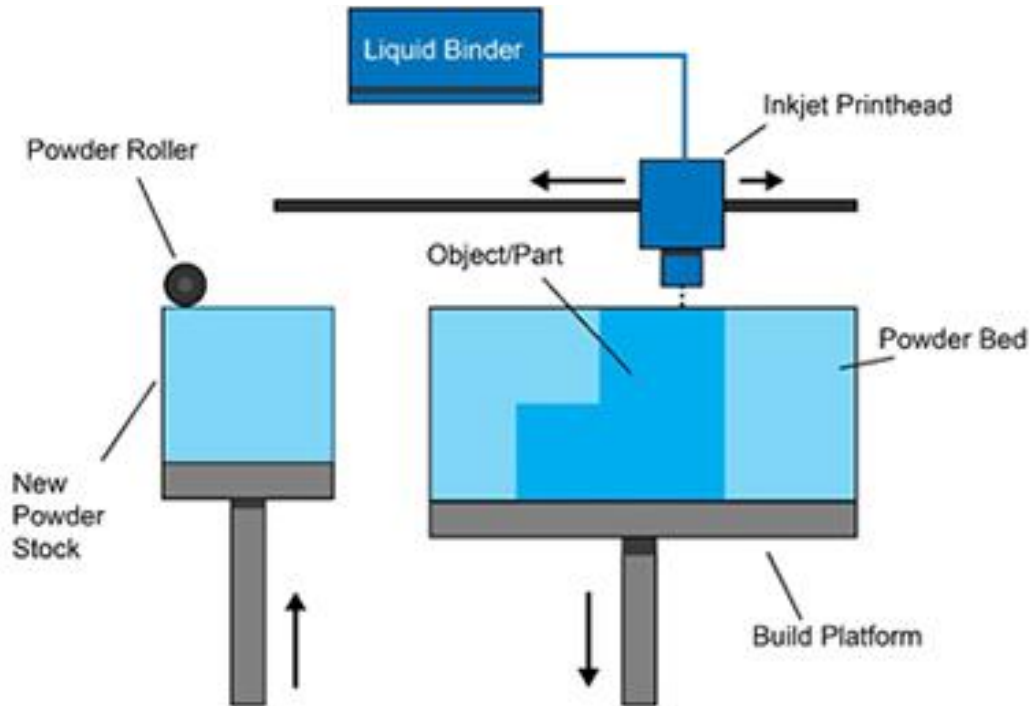


Figure 1.2 – Binder jetting [5].

DED deposits material that is then melted onto the surface of an already existing component. This process is only utilized to repair or add material to an already created part [6]. This process adds to the material layer by layer and this process is demonstrated in Figure 1.3. The only materials that are possible for this process are metals and this is because new material cannot be added to polymers or ceramics.

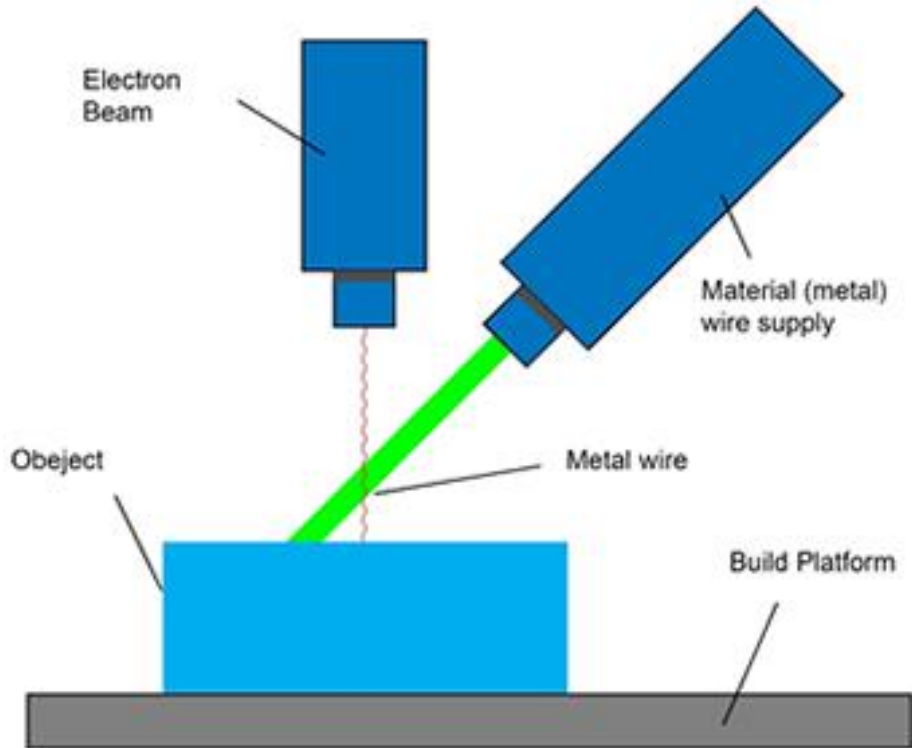


Figure 1.3 – Directed energy deposition [6].

ME has the material heated as it is pushed through a nozzle and then ejected onto a platform. This material is placed layer by layer to create the modeled component [7]. Figure 1.4 demonstrates the layout of the ME process. This process is only possible with the use of polymers and plastics as materials. The material fed through the nozzle needs to be constant during the whole process or the entire process will fail. The quality of this process is dependent on the size of the nozzle since some minute details are impossible.

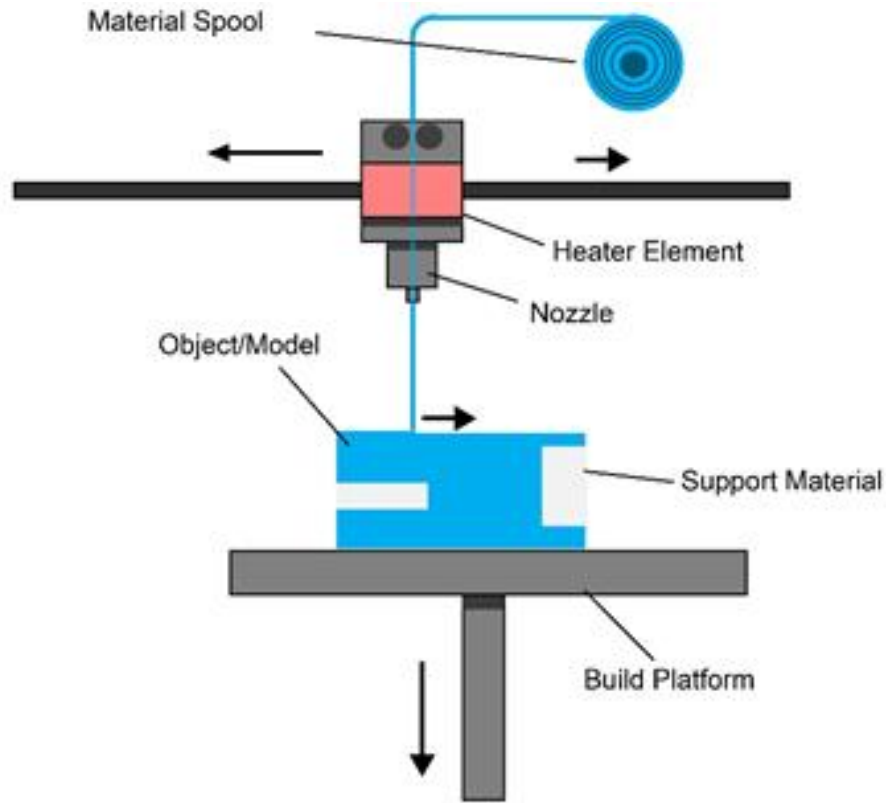
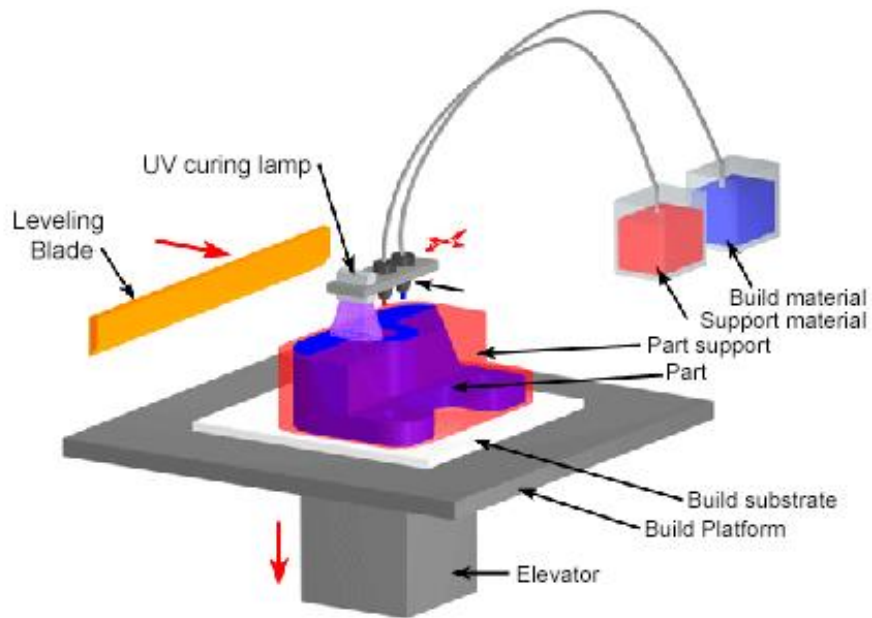


Figure 1.4 – Material extrusion [7].

MJ releases droplets of the material released onto a platform where it then solidifies by a UV light [8]. Figure 1.5 demonstrates the layout of a MJ process. This process is similar to how a printer places ink onto paper, but the material is instead solidified. Only polymers and plastics are possible materials for this process.



Copyright © 2008 CustomPartNet

Figure 1.5 – Material jetting [8].

PBF utilizes a laser or electron beam that melts and fuses powdered material layer by layer. After a layer is completed, the platform is then lowered to allow for a powder to be rolled over the already completed section [9]. This allows for minute control over the design since the thinnest the material can be is the diameter of the heat source utilized. The setup is demonstrated in Figure 1.6. The main material used in PBF are metals, but polymers can be used as well.

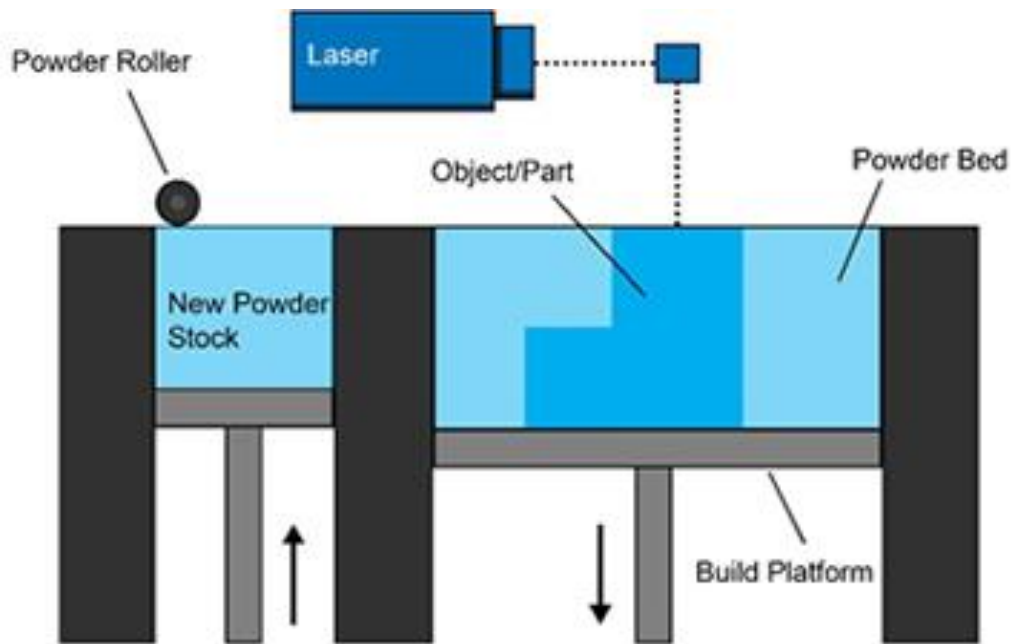


Figure 1.6 – Powder bed fusion [9].

SL layers thin sheets of material onto one another and are then bonded together through ultrasonic welding as shown in Figure 1.7. After the welding of each layer, the shape and unbonded material are cut by a laser and this process is completed for each of the layers. The materials available for this process are any that could be rolled up such as plastic or some sheets of metal.

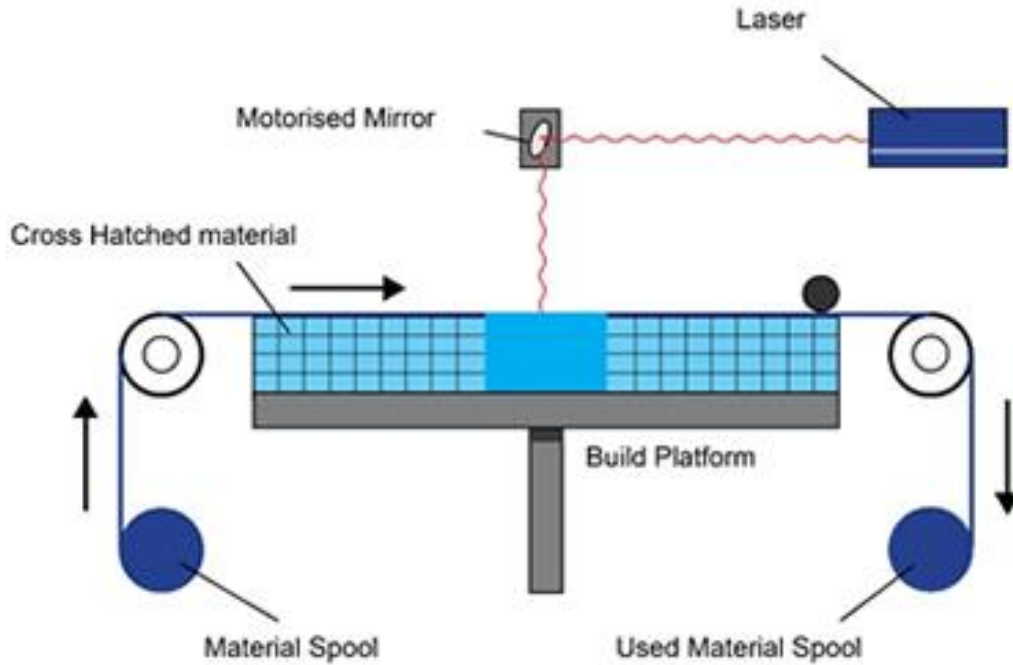


Figure 1.7 – Sheet lamination [10].

VP utilizes a tub of liquid material that the part will be made of and utilizes an ultraviolet light that hardens the necessary liquid for the part. After each layer is created, a platform moves the part lower so that the next layer can be created as shown in Figure 1.8. This process may need assistance from the user with adding support to the part when necessary, during the process. The only materials that can be used in this process are plastics and polymers.

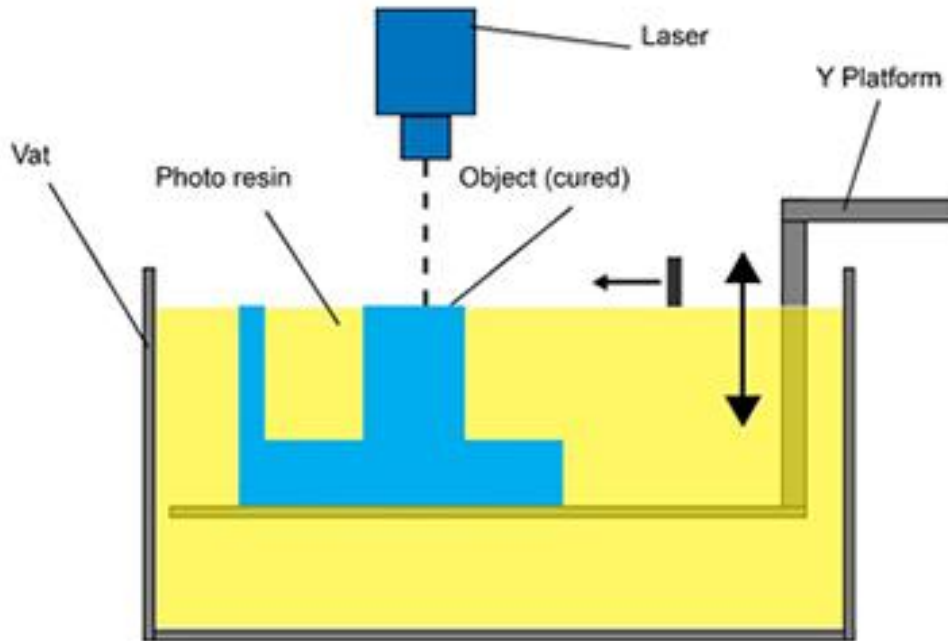


Figure 1.8 – Vat photopolymerization [11].

AM processes are already being implemented into current designs for CubeSats, but most are only focusing on the different systems of the CubeSat such as the structure, antenna, or mechanisms within the CubeSat.

In an article titled “Additively manufactured mirrors for CubeSats” written by Carolyn Atkins and associates, they demonstrate a UK Space Agency (UKSA) funded project that designs and manufactures AM mirrors that would fit within a 3U CubeSat chassis [12]. The authors are looking into using AM for mirrors since this would allow for a lightweight but optimized design.

Another article titled “An additive manufactured CubeSat mirror incorporating a novel circular lattice” by Robert Snell and associates, revises AM for mirrors on CubeSats as well but focuses on the use of a lattice integrated into the structure of the mirror. This lattice structure is designed to create a lightweight mirror that would then increase the design freedom [13]. The authors would then be able to experiment with designs that have not been possible to test before.

In “Selective Laser Melting of a 1U CubeSat structure. Design for Additive Manufacturing and assembly” written by Alberto Boschetto and associates, focuses solely on redesigning the structural subsystem for CubeSats. They are utilizing AM since this would give them access to design that would be otherwise unobtainable if subtractive manufacturing was utilized [14]. The redesign is geared towards consolidating parts so that the result created is the least number of parts possible.

An article titled “3D-Metal-Printed 60 GHz Offset Dual-Reflector Antenna with Integrated Conical Feed Horn and Circular-to-Rectangular Waveguide Transition” written by Ruben Sanches and associates, covers an antenna that is an inter-satellite between CubeSats that are designed to be created through AM processes. The authors were successful in designing and manufacturing a

metal AM antenna and the results show progress in AM being used for high-gain antennas [15]. This successful experiment demonstrates how utilizing AM in different aspects of CubeSats can result in positive results for that subject.

An article titled “Design and optimization of a multifunction 3D-Printed structure for an inspector CubeSat” written by Terry Stevenson and associates looks over incorporating the propulsion system of a CubeSat into the hollow spaces within the structure. This includes the propellant tanks, feed pipes, and thruster nozzles that will be modified into a single part with AM [16]. The authors are incorporating the important aspects of a propulsion system into a singular piece that affects each of the other subsystems of a CubeSat since its overall weight of it would decrease.

1.3 Project Proposal

The objective of this master’s project is to design a two-by-three 6U (1U is 10 cm x10 cm x 11.35 cm) CubeSat where the propulsion system is integrated into the structural support system. When these two structures are combined into one, the CubeSat should have a decrease in overall weight. The entire structure will be designed to be created through the additive manufacturing method known as powder bed fusion.

1.4 Methodology

This project begins with researching the propulsion systems that are utilized in CubeSats that orbit the Earth. The type of propulsion system chosen will be modified into a single piece. Since the propulsion system and CubeSat structure will be manufactured through additive manufacturing, all aspects will have to be attached. The propulsion will then be designed in CAD and designed to be a single part. The structure will then be designed around the propulsion system. The program used to model the design will be Inventor since this is the program that I have the most experience with. Once the complete structure is completed, then simulations will be completed to test the validation of building it and its different capabilities. Based on these results, the design may be changed if the results of the simulations are not the desired ones. Once the changes are completed, the simulations are run again, and this cycle continues until the results are desirable. Then the results of the design are compared to the capabilities of a CubeSat that is sent into orbit around Earth.

2. CubeSat Design

2.1 Structure

The Advanced Propulsion Integrated within Structure (APIS) CubeSat structure is designed to fit the 6U design of a CubeSat. This was chosen to allow the necessary space for the propulsion system as well as sufficient room for two other payloads. These payload bays will have around 2U of space each. One of the payload bays will contain the flight systems for the CubeSat which includes the flight computer, power supply, etc. This system is envisioned to fit within only 1U of space within a payload. The propulsion system is placed in the center of the CubeSat so that the overall center of gravity is close to the center of the CubeSat. This design is considered so that the moment created from the propulsion of the thrusters is the same no matter which thruster is utilized. The first iteration of the structure with the propulsion system is shown in Figure 2.1. This design is in the premature stages and only has the purpose of demonstrating the locations of the propulsion system and the thrusters

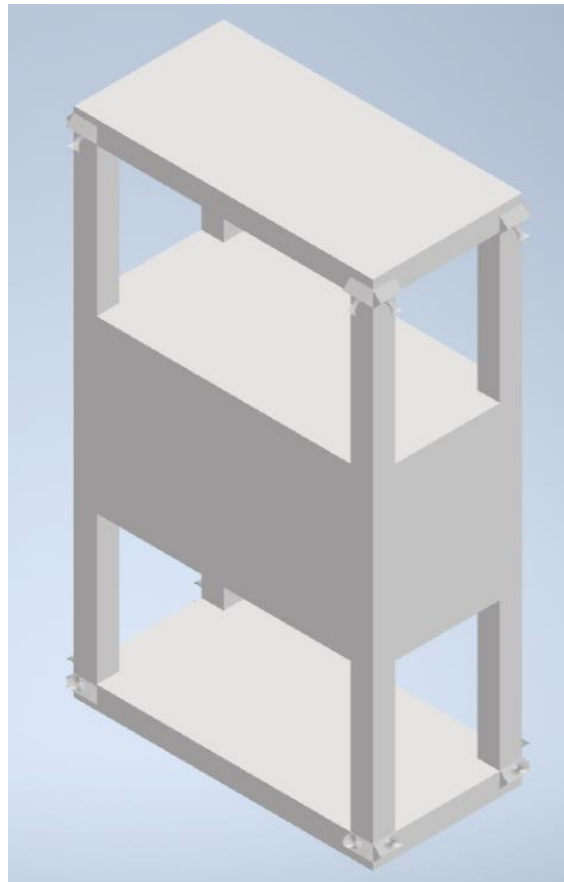


Figure 2.1 - First iteration of APIS.

The material designated for this design is aluminum since the additive manufacturing method chosen is PBF. The alloy of aluminum chosen is AlSi10Mg since it is commonly used in additive manufacturing. This specific alloy has characteristics of lightweight and good thermal conductivity [17]. The choice of additive manufacturing is based on how two systems of the CubeSat can be manufactured into a singular piece and still function at the desired capabilities.

This method as well as the desired tolerance is only available with this method while utilizing the desired material.

2.2 Skeletal Structure

The surrounding structure for APIS is designed to add support for the inner components of it excluding the propulsion system. This additional material will be lightweight because of a lattice structure design that allows for less material utilized while being able to contain the inner components. A lightweight design is desired since APIS is designed to be as light as possible. This lattice will be similar to the two main faces of APIS while the smaller faces will be more open so specific inner components can be swapped as desired. Even though the faces will have less material than a solid face, there will be panels placed on each side to protect the inner components and add additional strength to the structure that could be lost due to the lattice structure. These panels will be manually screwed onto the skeletal structure of the CubeSat.

Certain sections will be customizable for APIS since they could be used for any type of mission. This type of accessibility allows APIS to accommodate missions that utilize a bunch of smaller subsystems while allowing for the larger subsystems as well. Figure 2.2 demonstrates the different sections of APIS that will be customized based on the mission.

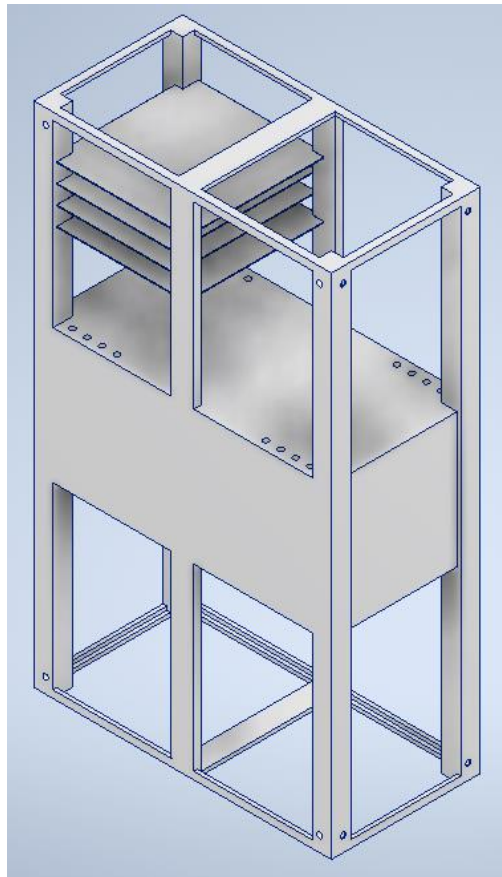


Figure 2.2 – Second iteration of APIS.

2.3 Propulsion

The APIS CubeSat propulsion system will utilize cold gas which will propel the CubeSat using the pressurized propellant stored within the propulsion system. This simplifies the complexity of the propulsion system since there is no need to create thermal protection in the propulsion system from the heat that would be generated from combustion. The tanks for the propellant will be interchangeable tanks that will increase the reusability of the CubeSat for multiple missions. The exact number of these tanks is not decided yet but is going to be two to four total tanks. The propellant chosen for this propulsion system is CO₂.

The system is designed with sixteen thrusters to total a grouping of two on each corner of the structure. Each thruster is facing toward the center of the CubeSat with an angle of 45°. This number of thrusters is designed to allow the CubeSat to easily control the attitude and rotation during its future missions. The micro fluidity channel that allows for the propellant to reach the thrusters will be designed into the main four corners. This integration of the propulsion system into the structure will allow for the maximum space available for the payloads as well as decrease the overall weight of the CubeSat.

The CAD design in Figure 2.3 demonstrates the piping of the propulsion system that is going to be within the structure of the CubeSat. The storage tank of the propulsion system is piped to the valve manifold where it is then connected to the propulsion piping that leads to the thrusters. The valve manifold will control how much of the propellant is released and in which piping the propellant will be released. There will be a total of two valve manifolds with one on top of the propellant tank and one on the bottom. There will be a total of sixteen channels in each manifold where two channels will control a path from the tank to the thruster. This will be controlled by the electronic system that would be later designed into the CubeSat.

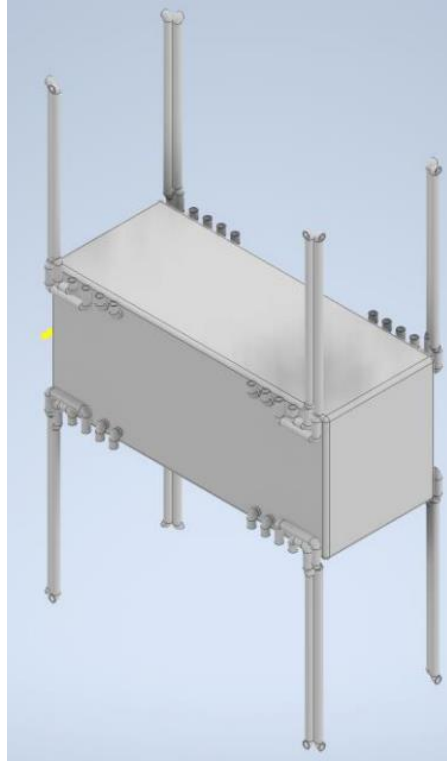


Figure 2.3 – Piping for the propulsion system.

The thrusters that are within the same corner of the structure will have a similar length for the propellant to travel within and each of the eight corners of the CubeSat will have the same piping path within each of them. Each corner of the CubeSat will have two thrusters with each being placed near the center of each of them. Since the piping is located within the support structure of the CubeSat, it does not interfere with the other compartments of the CubeSats and allows those spaces to be utilized to their max. This structure is only possible due to additive manufacturing processes because of the piping shown in Figure 2.3. This piping has intricate pathing that is impossible to complete in subtractive manufacturing due to it being within the structure.

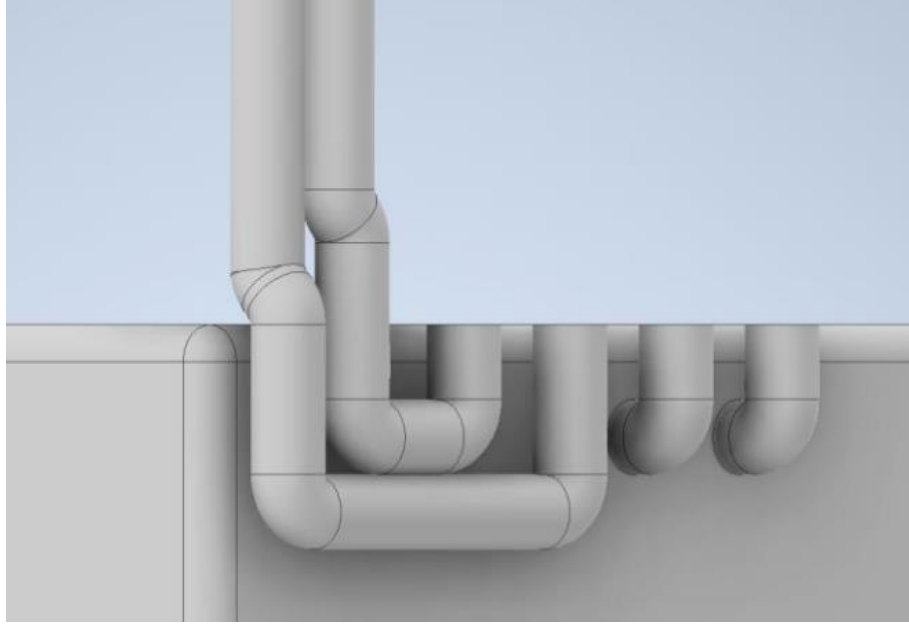


Figure 2.3 – Zoom in on piping.

3. CubeSat Launcher

3.1 CubeSat Launcher

APIS will have to fit within the specifications of a 6U CubeSat launcher designated by NASA. The size requirement designates a rail on each corner of a CubeSat with a length, width, and height respectfully being 100 mm (3.037 in), 226.3 mm (8.909 in), and 366 mm (14.409 in). The rails are each 8.5 mm (0.334 in) by 8.5 mm (0.334 in)[18]. These dimensions are shown in Figure 4.1. The only components that are allowed to be in contact with the CubeSat launcher are the rails. This means that the thrusters will not be able to expand past the limits of the launcher.

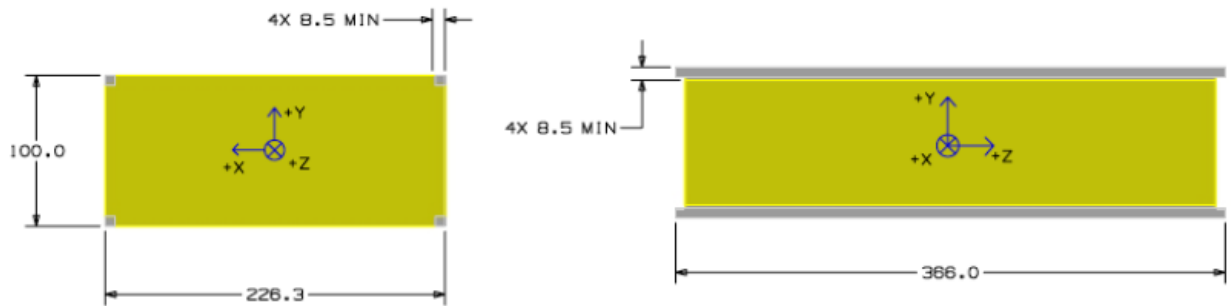


Figure 3.1 – Dimensions for CubeSat launcher [18].

Besides the dimensions, multiple testing requirements will have to meet the launch provider requirements. These tests include random vibration, thermal vacuum bakeout, shock testing, visual inspection, and CubeSat Testing Philosophy. Most of these tests are defined by the Mission Integrator except for the Visual Inspection and CubeSat Testing Philosophy. The Visual Inspection is only the measurement of critical areas of the CubeSat. The CubeSat Testing Philosophy is a “conservative test flow approach for CubeSats to meet environmental test requirements for launch. The CubeSat shall be subjected to either qualification or protoflight testing as defined in the CubeSat Testing Flow Diagram” [18]. An example of this diagram is shown in Figure 3.2.

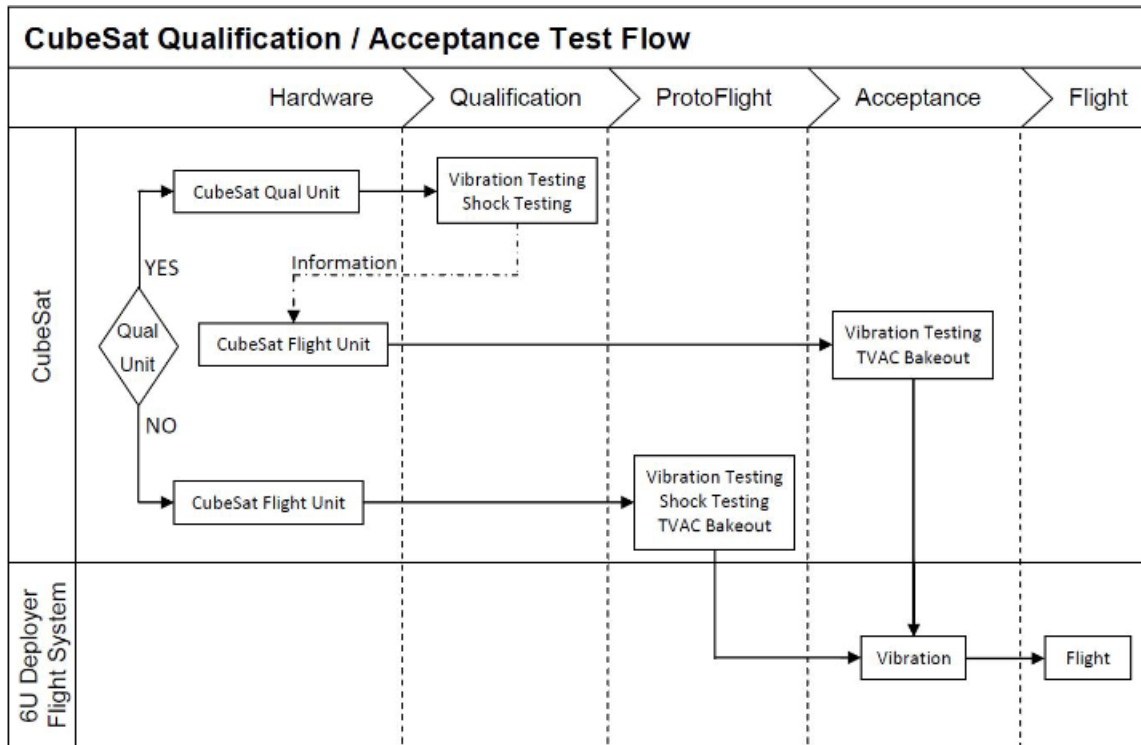


Figure 3.2 – CubeSat General Testing Flow Diagram [18].

The qualification testing is performed on a unit that is identical to the flight model CubeSat which would be APIS and this determines the Mission Integrator. The flight model is assessed at the acceptance levels in a Test 6U Dispenser. It will then be integrated into the flight 6U dispenser for a random vibration test as the final verification. There may be additional testing necessary if changes or modifications are made to the CubeSat after qualification testing.

The protoflight testing is only applied to the flight model CubeSat. This model is assessed at protoflight levels in a Test 6U Dispenser and then integrated into the flight 6U dispenser for a random vibration test that is the final verification. The flight CubeSat cannot be taken apart or modified at all after the protoflight test. If there is a modification, then the Mission Integrator is informed and determines the next steps.

4. Communication

4.1 Antenna

The antenna system will be located in the top two compartments of APIS with a total of four wire antennas that will be deployed on each side of APIS. The antenna will be equipped with a VHF/UHF (Very High Frequency/ Ultra-High Frequency) receiver whose frequency bands are 30-300 MHz and 300-1000 MHz respectively. Figure 4.1 shows the location of the four antennas when they will be fully deployed. The antenna extended shown in black in Figure 4.1 is a tape spring that is originally rolled up during launch shown in Figure 4.2. Each four of the antennas will be deployed at the same time so that the force exerted from the release of the tape spring will cancel each other out. The antenna wire is embedded within the tape spring to allow the antenna to easily deploy when necessary.

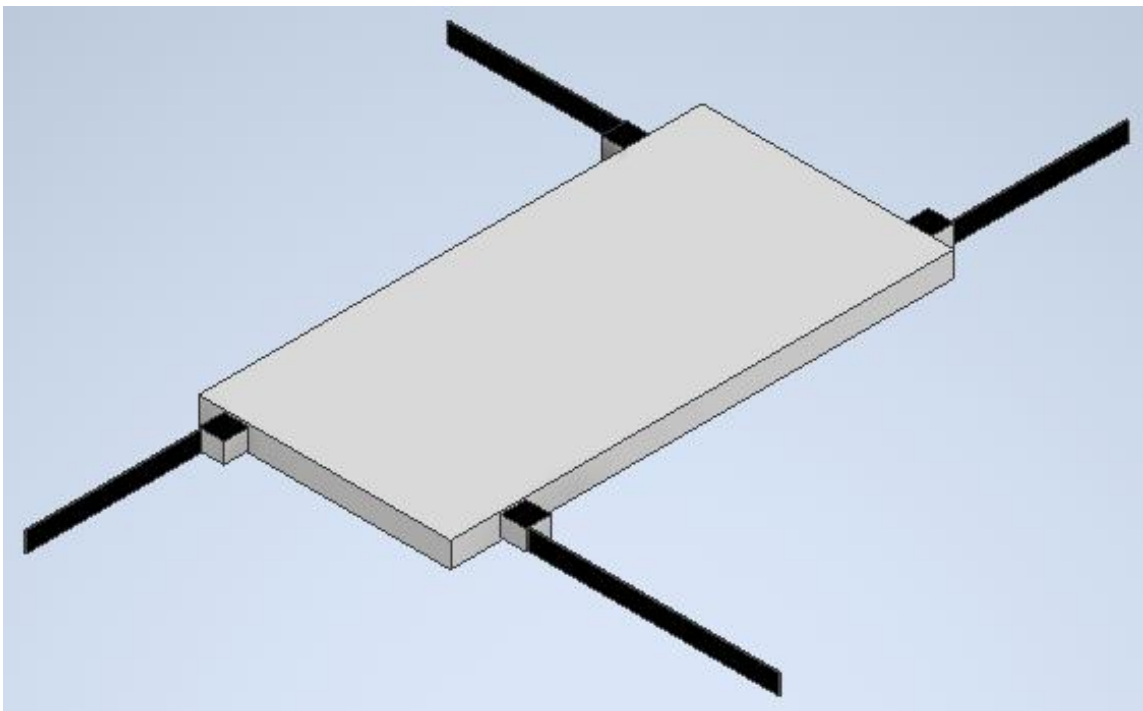
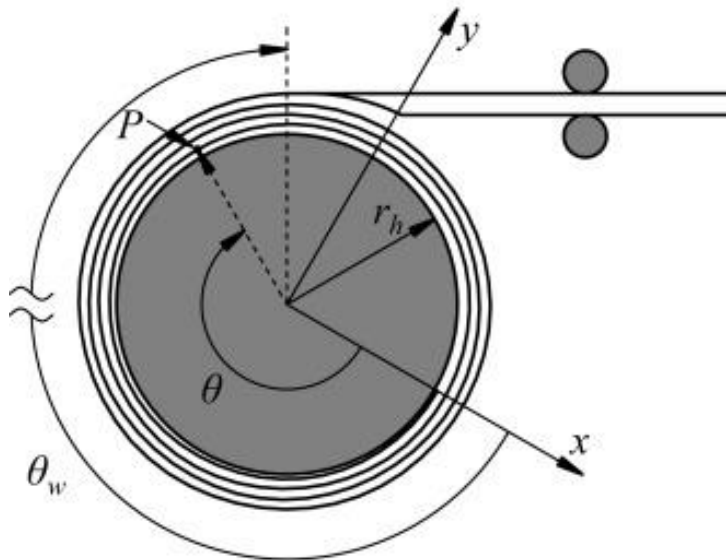


Figure 4.1 – Layout of four wire antennas.



(a) initial coil geometry

Figure 4.2 – Tape spring rolled up [19].

The mission requirements for an antenna as written by journal authors Sining Liu and coauthors should focus on telemetry, tracking and command, high-speed downlink for payload data, GPS and GNSS signal reception, and inter-satellite communication links [20]. These different requirements will change depending on the desired mission for the CubeSat but are achieved through this design with the VHF/UHF receiver that allows for reliable transmission and reception at the lowest possible volume.

5. Power System

5.1 Battery

CubeSats have two batteries: the primary battery and the secondary battery. The primary battery is non-rechargeable and is used in a one-time short use. It is normally used during or shortly after launch but can also be used over extended periods in short bursts. These batteries have a higher power density and a wider range of operating temperatures. The most common type of battery used within CubeSats is Lithium-based.

The secondary battery is utilized for most of the duration of the mission since the demand necessary for the whole mission is greater than the capabilities of the primary battery. Lithium-based batteries are also the most utilized type of battery for CubeSats.

The main requirements for batteries are the peak power requirements, worst-case orbit energy requirement, operating temperature, and mission life. These requirements are used to determine the cells that are necessary for the mission and then a combination of cells is combined to form a battery pack. The common dimensions of battery cells are 18 mm (0.708 in) in diameter and 65 mm (2.559 in) in height [21]. These have been chosen due to their small size while being able to operate within space conditions.

5.2 Solar Panels

The solar panels are designed on the four panels surrounding the CubeSat that will protect the inner compartments. This design was chosen because no matter which side faces the sun, it will have solar panels there. This was also chosen because it would reduce the need to use the propulsion system to rotate the CubeSat so that the solar panels could face the sun.

Each panel will have multiple panels on them instead of a singular one that would cover the entire panel. This is so that in case of an instance of a panel malfunctioning, the entire solar panel will not be out of commission, instead only a singular panel will not work while the rest of that panel will work fine. This spacing of the solar panels is shown in Figure 5.1 with the black section as the location for solar panels. The left panel is for the front and back of the CubeSat while the right one is located on both sides. There will be a total of 24 solar panels placed around the CubeSat.

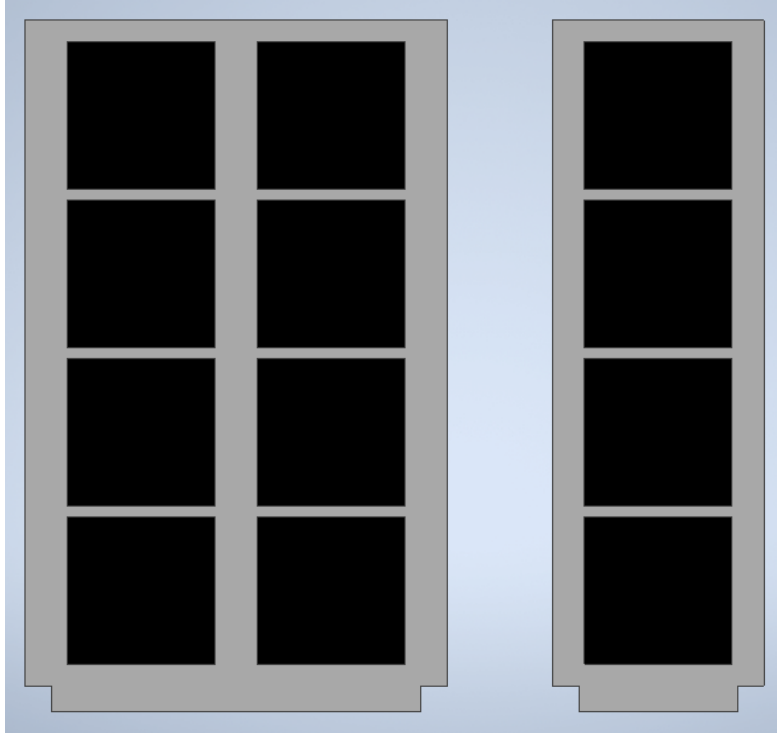


Figure 5.1 – Panels with solar panels.

6. Analysis

6.1 Finite Element Analysis

The Finite Element Analysis (FEA) within Inventor was utilized to predict how APIS will respond to the loads that it would experience during the launch. After FEA completes, there will be a color scale shown that shows the max and min of the results of the analysis. An example would be the displacement of the part based on the forces applied to it.

This analysis will focus on the loads that APIS will experience and will utilize the specific loads that a payload aboard the Falcon 9 rocket would experience. The *Falcon User's Guide* which is a manual that is given to the customers of SpaceX displays the load factors that a payload under 4,000 lb (1814.369 kg) will experience [22]. Figure 6.1 shows this image from this manual of the load factors for a payload under 4,000 lb (1814.369 kg) in red while the black load factors are for the rest of the payloads.

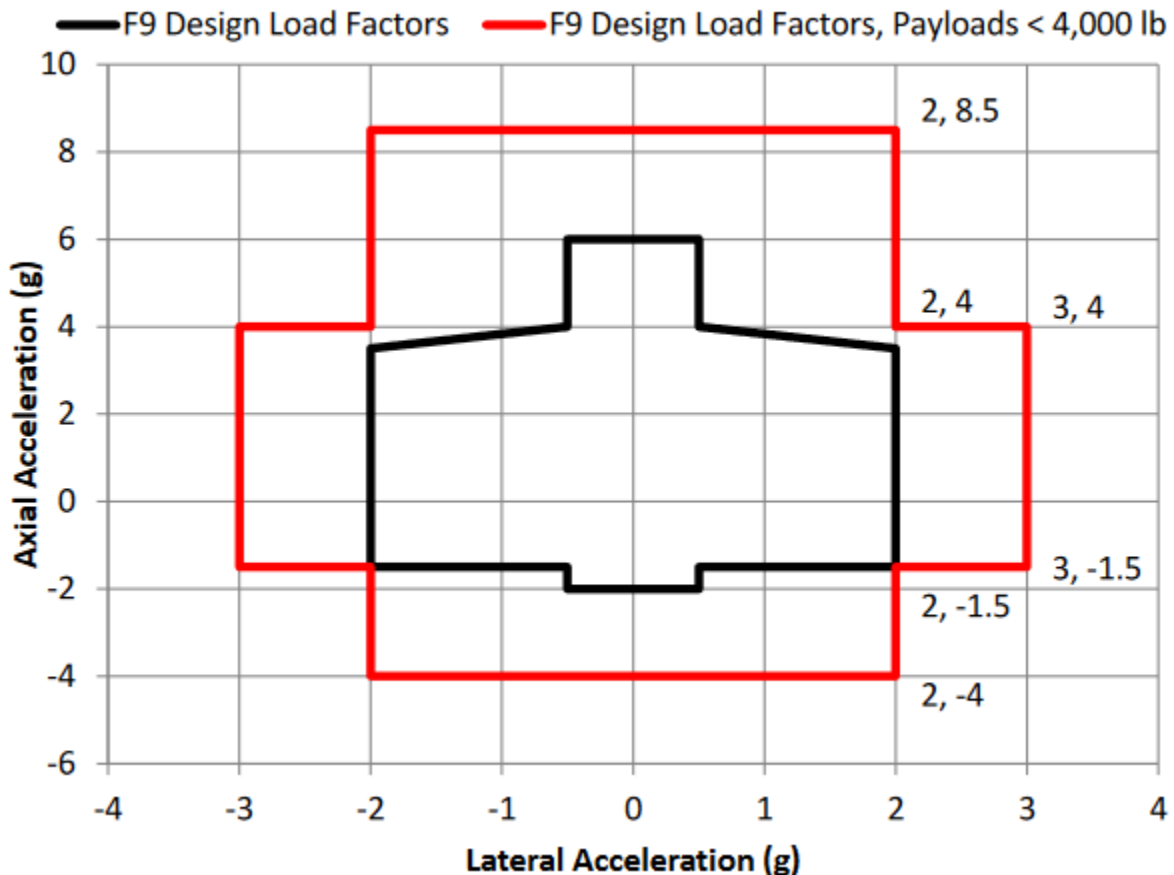


Figure 6.1 - Load Factors for Falcon 9 rocket.

These load factors are given in the units of g's which is gravity. The force equation as shown in equation 6.1 will be used to calculate the forces that APIS would experience if it was a payload for the Falcon 9 rocket.

$$F = m * a \quad (6.1)$$

The mass of the CubeSat structure is estimated to be around 2.388 kg (5.264 lb) from using the mass given by Inventor with the density of AlSi10Mg. The FEA will be completed with two pairs of load factors that are shown to be the extremes of what a payload aboard Falcon 9 rocket would experience. These two extreme pairs of load factors are 2 and 8.5 and 3 and 4 of the lateral and axial acceleration respectively. The forces that will be applied to APIS are calculated to be 4.776 N (1.073 lbf) and 20.298 N (4.563 lbf) for the first pair. The second pair was calculated to be 7.164 N (1.610 lbf) and 9.552 N (2.147 lbf). The FEA completed on APIS will have the lateral acceleration force applied to the larger front face of APIS in the z-direction shown from the model while the axial acceleration force is applied to the shorter side face of APIS in the x-direction. The top and bottom of APIS are set as a fixed constraint which keeps faces locked in place while the forces are applied to the z and x directions. Figure 6.2 shows the displacement for the first pair of lateral and axial acceleration forces and Figure 6.3 shows the second pair.

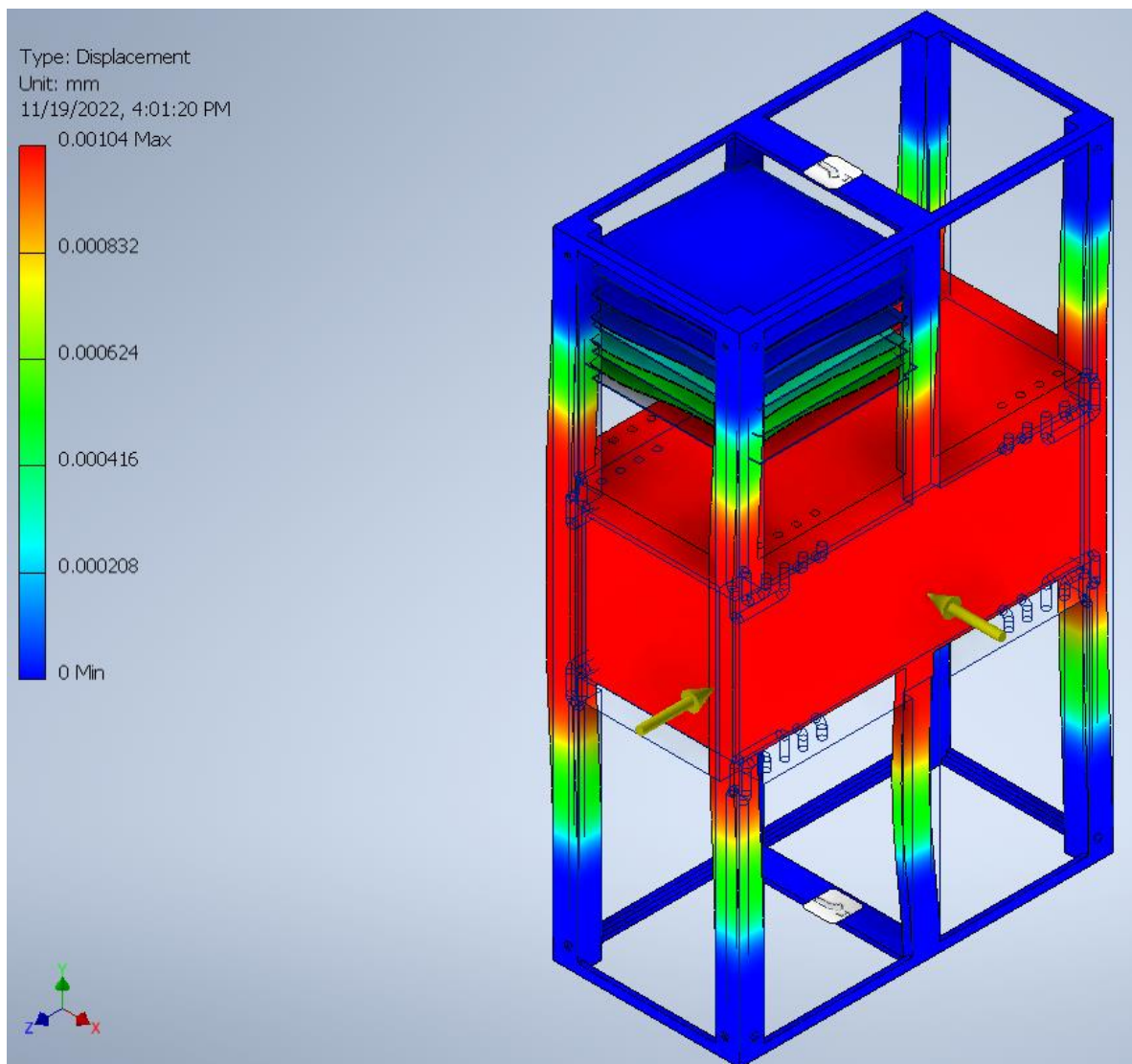


Figure 6.2 – Displacement for the first pair.

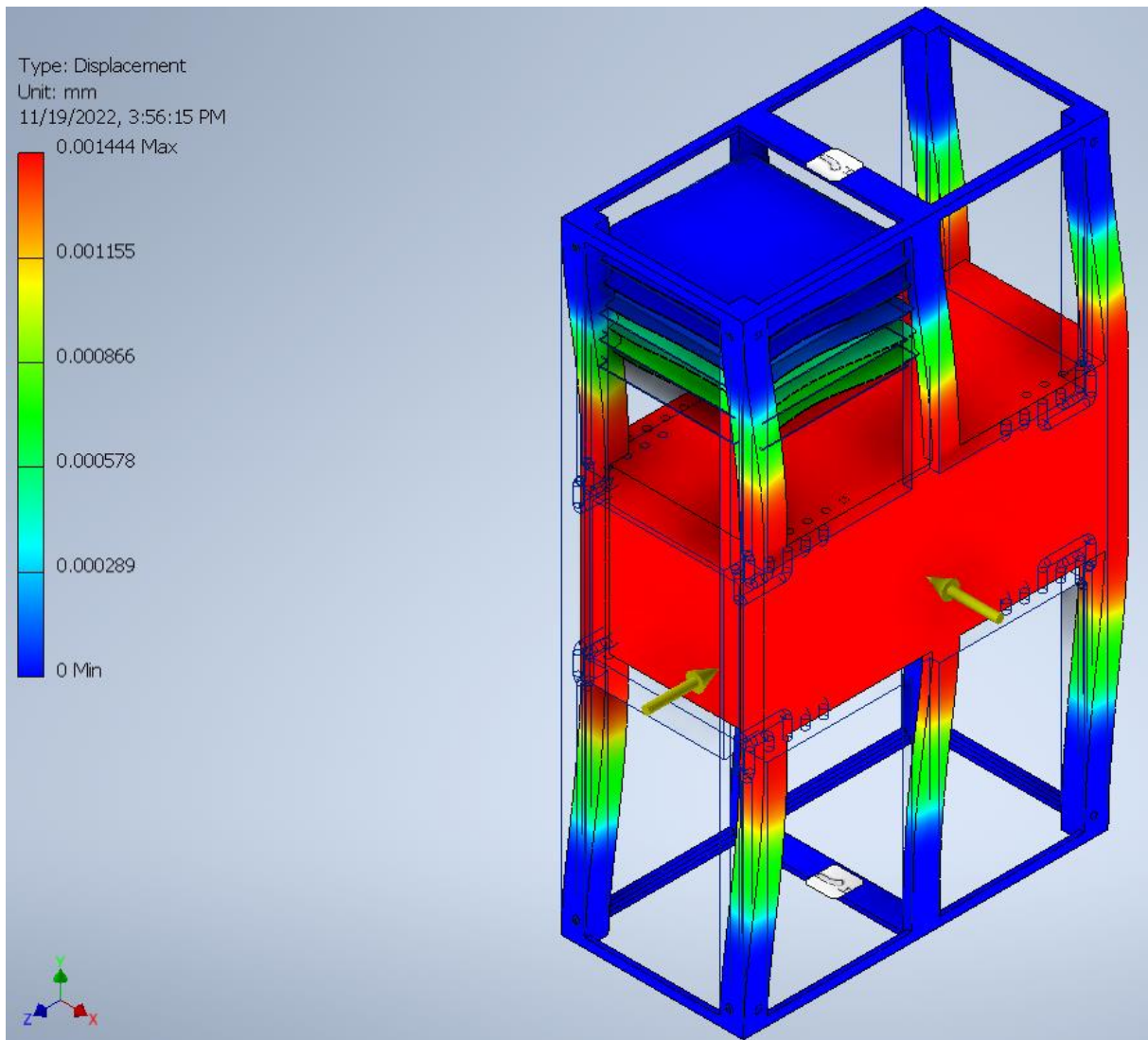


Figure 6.3 - Displacement for the second pair.

The displacement shown in Figure 6.2 has a max displacement of .00104 mm ($4.094E-5$ in) while Figure 6.3 has a max displacement of .001444 mm ($5.685E-5$ in). This difference shows that the face in the x-direction is more vulnerable to external forces during launch since the lateral acceleration force for the second pair is .5 times larger than the first pair while the axial force decreased by more than half from the first axial acceleration force to the second.

The safety factor for APIS was also calculated during the FEA in Inventor. Figures 6.4 and 6.5 show the safety factors calculated for both pairs. Both have the same safety factor of 15 across APIS. This high number shows that the structure is still viable even after the forces are applied to it. A lower number for the safety factor would mean that the structure is compromised and would not be reliable in the future.

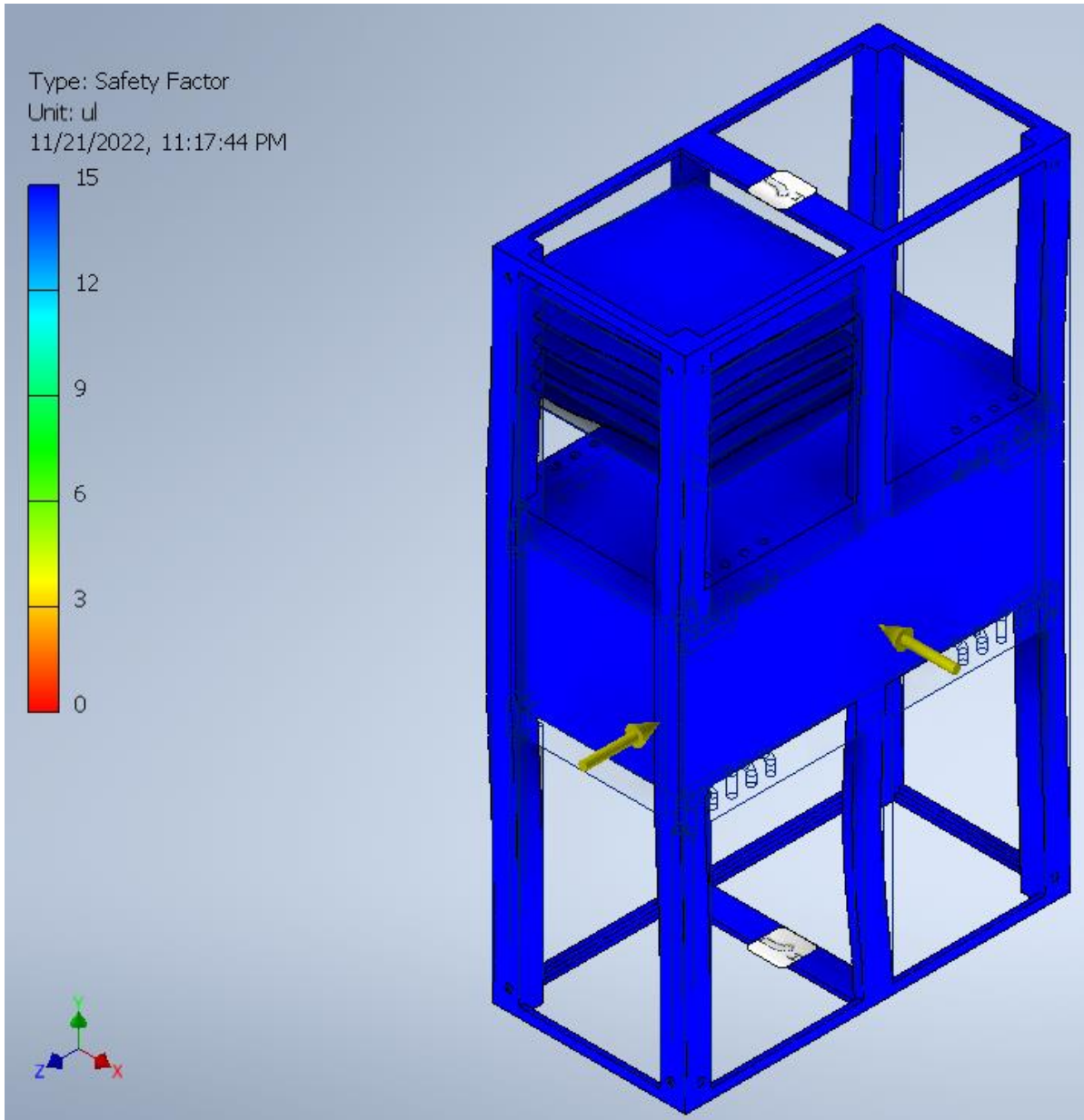


Figure 6.4 - Safety Factor for the first pair.

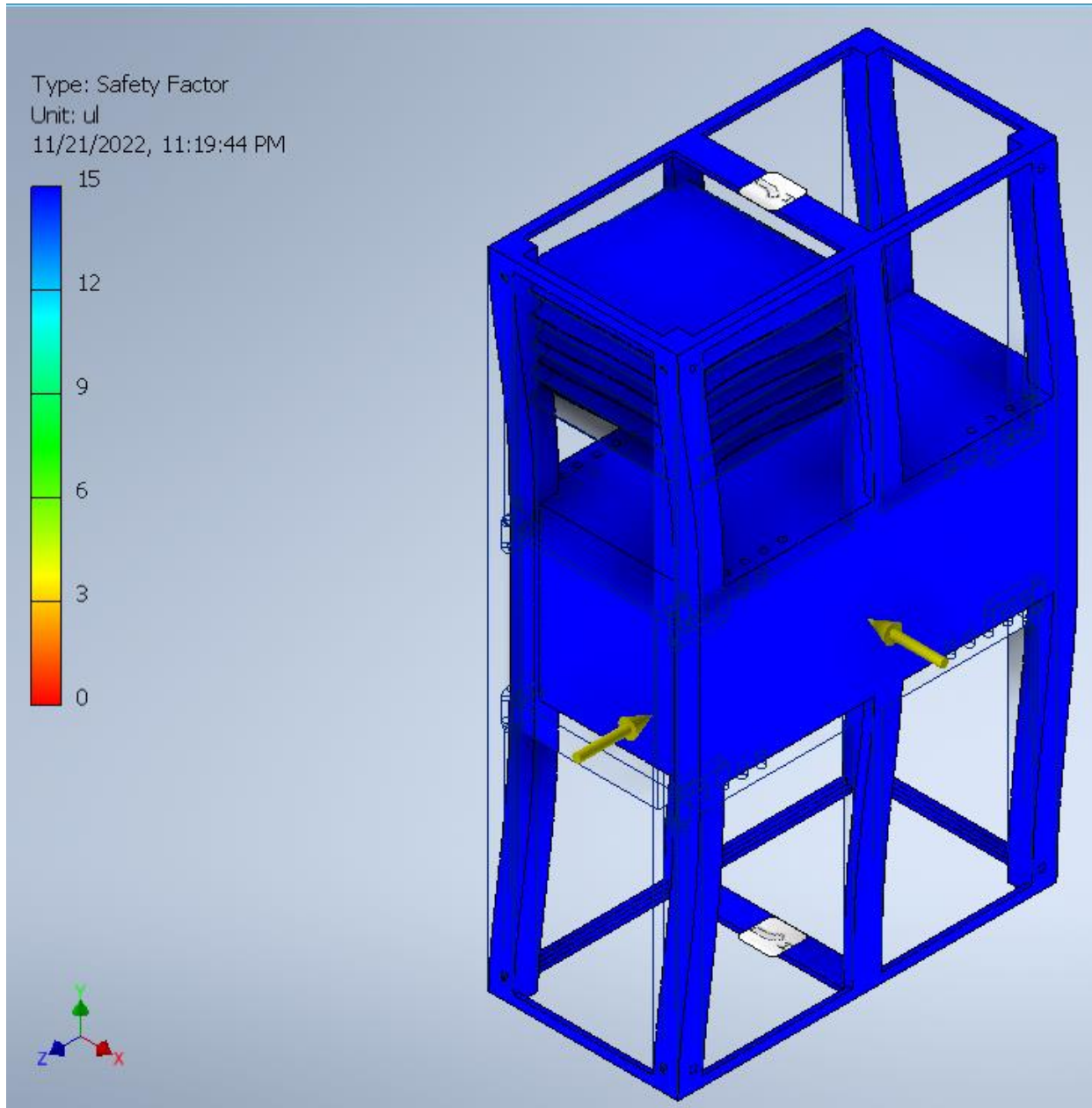


Figure 6.5 - Safety Factor for the second pair.

The Von Mises Stress is the next aspect of the FEA calculations from Inventor and is shown in Figures 6.6 and 6.7. This stress is used to determine if the material tested either yields or fractures. Yield is the occurrence where the forces on the material exceed its elastic limit and causes permanent deformation in the material. This will lead to a reduction in the integrity of the material. Both Von Mises Stresses shown from both pairs of forces applied to APIS show that neither of them reaches the point of fractures or yields.

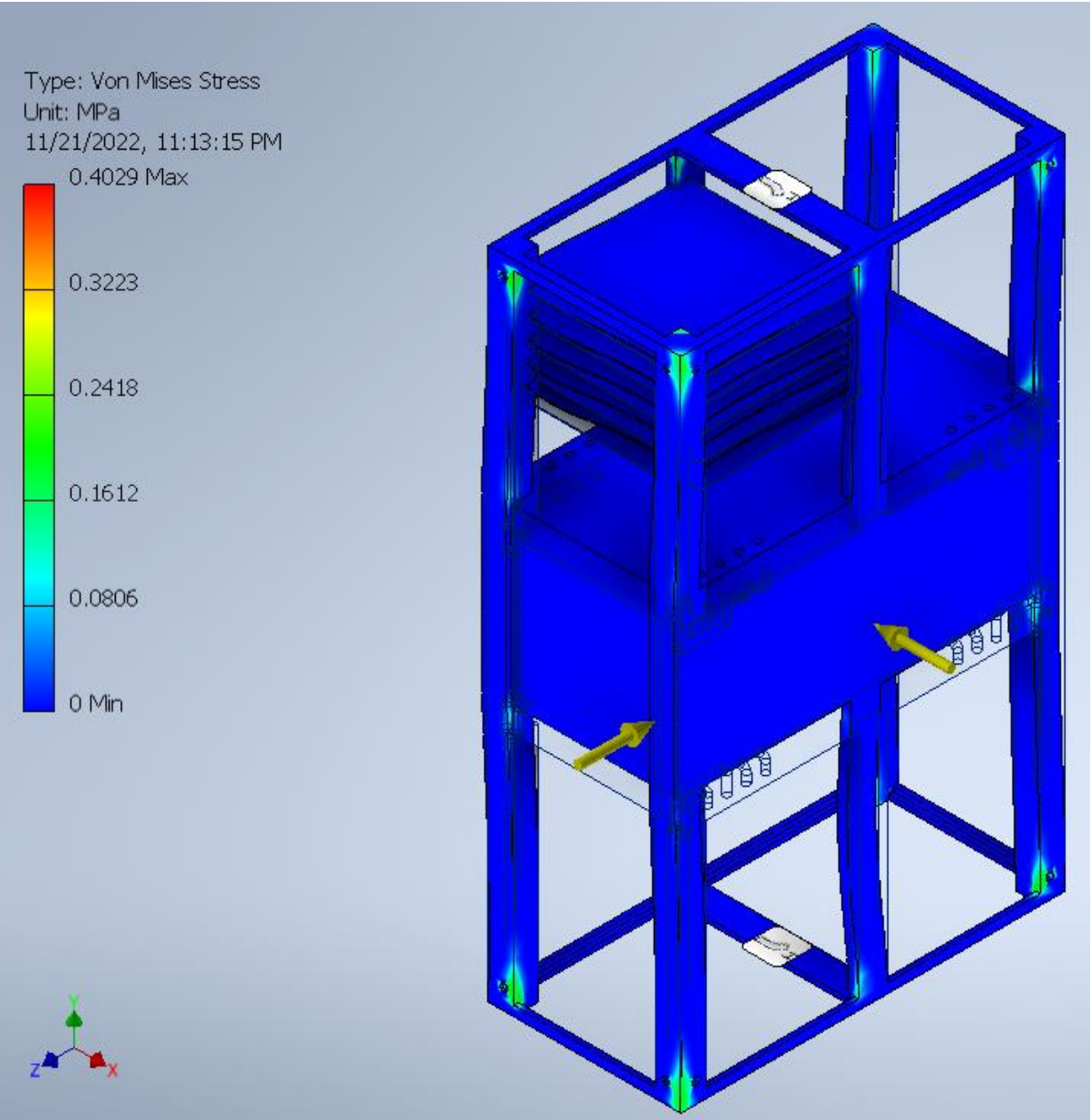


Figure 6.6 - Von Mises Stress for the first pair.

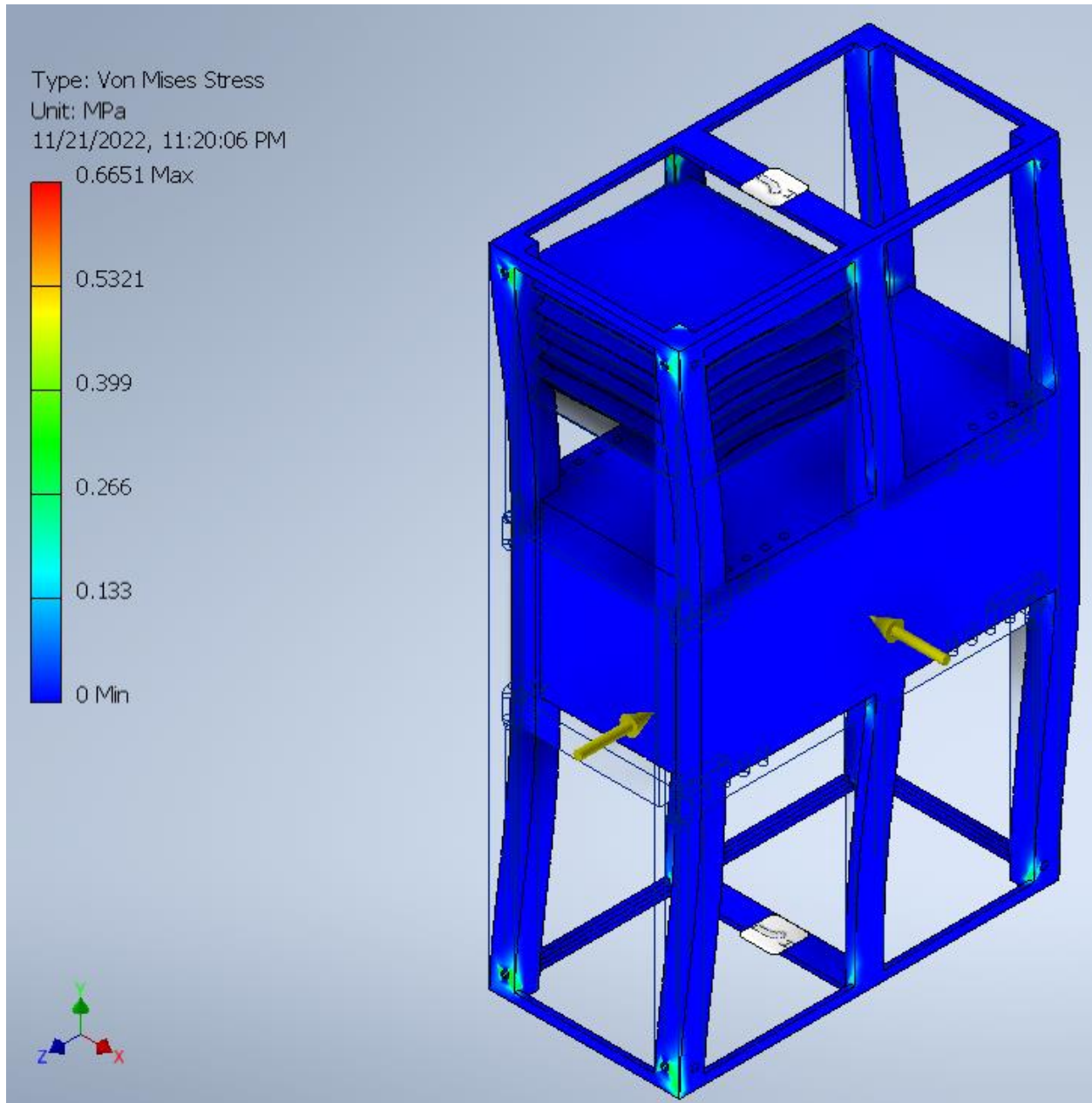


Figure 6.7 - Von Mises Stress for the second pair.

These analyses of the APIS structure demonstrate how it will still be functional and fully operational after it experiences the loads it would experience during the launch into space. This is especially necessary since if APIS got damaged during the launch, then it would be meaningless to launch it into orbit since it would not be able to complete its desired mission.

6.2 Thrust Analysis

The thrust force, shown in equation 6.2, will be calculated using a series of equations gathered from the NASA website [23]. Since APIS will be in Earth's orbit, the thrust can be

assumed to be in a vacuum, so the thrust equation becomes equation 6.3 where the pressure equations are ignored and the focus is on the exit velocity and the mass flow rate.

Thrust equation:

$$F_T = \dot{m} * V_e + (P_e - P_a) * A_e \quad (6.2)$$

Thrust equation in a vacuum:

$$F_T = \dot{m} * V_e \quad (6.3)$$

The exit velocity equation 6.5 is gathered from the exit Mach number equation shown in equation 6.5. The missing variables of exit Mach number and exit temperature are found in equations 6.6 and 6.9 respectively. The exit Mach number equation is derived by rearranging the area ratio in equation 6.7 and this derivation is shown in Appendix A.

Exit Velocity equation:

$$V_e = M_e * \sqrt{\gamma * R * T_e} \quad (6.4)$$

Derived from the Mach number equation:

$$M_e = \frac{V_e}{\sqrt{\gamma * R * T_e}} \quad (6.5)$$

Exit Mach number equation:

$$M_e = \sqrt{\left(1 + \frac{\left(\frac{A_e}{A^*}\right)^2 - 1}{2 * \left(\frac{\gamma}{\gamma+1}\right)^{\frac{\gamma+1}{\gamma-1}}}\right) - \sqrt{\left(1 + \frac{\left(\frac{A_e}{A^*}\right)^2 - 1}{2 * \left(\frac{\gamma}{\gamma+1}\right)^{\frac{\gamma+1}{\gamma-1}}}\right)^2 - 1}} \quad (6.6)$$

Derived from the Area ratio:

$$\frac{A_e}{A^*} = \left(\frac{\gamma+1}{2}\right)^{-\frac{\gamma+1}{2 * (\gamma-1)}} * \frac{\left(1 + \frac{\gamma-1}{2} * M_e^2\right)^{\frac{\gamma+1}{2 * (\gamma-1)}}}{M_e} \quad (6.7)$$

The velocity equation requires the exit temperature, and this is taken from the temperature ratio in equation 6.9 and becomes equation 6.10.

Temperature ratio:

$$\frac{T_e}{T_t} = \left(1 + \frac{\gamma-1}{2} * M_e^2\right)^{-1} \quad (6.8)$$

becomes,

$$T_e = T_t * \left(1 + \frac{\gamma-1}{2} * M_e^2\right)^{-1} \quad (6.9)$$

The values for all the necessary variables for equations 6.2 - 6.12 are shown in table 6.1 and the results of the input data into the equations are shown in table 6.2.

Table 6.1 - Nozzle and throat data.

Parameter	Value
Ae	.005 m (.000196 in)
A*	.001 m (.0000393 in)
γ	1.289
Tt	230 K (-43.15 °C)
R	188.9 J/kgK (1130 ft lb/slug °R)
ρ	1.87 kg/m ³ (6.755E-5 lb/in ³)
\dot{m}	.0001 kg/s (.00022 lb/s)

Table 6.2 - Equation results.

Parameter	Value
Me	.1179
Ve	27.88 m/s (91.469 ft/s)
Te	249.21 K (-24.15 °C)
Ft	.02788 N (.00626 lbf)

The resulting calculated thrust force value is 27.88 mN (. This result of the thrust force is an acceptable result when comparing this to the thrust force of CubeSats such as Mars Cube One (MarCO) which had a thrust of 50 mN (.0112 lbf) [25]. MarCO is a twin communications-relay CubeSat designed by NASA's Jet Propulsion Laboratory that was designed to carry out experiments that focused on communication and navigation as they flew by Mars [26]. These CubeSats were of similar size to APIS by being 6U CubeSats.

Since APIS has a total of sixteen thrusters, where each can produce around 27 mN (.00606 lbf) of thrust, it will be fully able to rotate as desired for the mission. If it is necessary to rotate for a condition of the mission or to optimize the solar panel placement with the sun, APIS will be able to complete this with these thrusters.

7. Conclusion

APIS can be the next step in improving the design of CubeSats. Integration of the propulsion system within the structure is shown to be a feasible step as shown by the analysis of the propulsion and the structure. The propulsion system is shown to be capable of producing a similar thrust to CubeSats of a similar size. The structure is shown to have the necessary durability that is needed to withstand the forces of being launched into space and still be capable of completing its desired mission. A CubeSat that will overall weigh less from the integration of the propulsion system into the structure while also being manufactured through additive manufacturing is a significant improvement when compared to a common CubeSat of similar size.

References

- [1] Howell, E. (2018, June 19). *Cubesats: Tiny Payloads, huge benefits for space research*. Space.com. Retrieved February 21, 2022, from <https://www.space.com/34324-cubesats.html>
- [2] Loff, S. (2015, July 22). *CubeSats Overview*. NASA. Retrieved February 22, 2022, from https://www.nasa.gov/mission_pages/cubesats/overview/
- [3] Mabrouk, E. (2015, March 13). *What are SmallSats and CubeSats?* NASA. Retrieved February 21, 2022, from <https://www.nasa.gov/content/what-are-smallsats-and-cubesats/>
- [4] Tofail, S. A. M., Koumoulos, E. P., Bandyopadhyay, A., Bose, S., O'Donoghue, L., & Charitidis, C. (2018). Additive Manufacturing: Scientific and technological challenges, market uptake and opportunities. *Materials Today*, 21(1), 22–37.
<https://doi.org/10.1016/j.mattod.2017.07.001>
- [5] Loughborough University. (n.d.). *Binder Jetting: Additive Manufacturing Research Group*. Loughborough University. Retrieved February 23, 2022, from <https://www.lboro.ac.uk/research/amrg/about/the7categoriesofadditivemanufacturing/binderjetting/>
- [6] Loughborough University. (n.d.). *Directed Energy Deposition: Additive Manufacturing Research Group*. Loughborough University. Retrieved February 23, 2022, from <https://www.lboro.ac.uk/research/amrg/about/the7categoriesofadditivemanufacturing/directedenergydeposition/>
- [7] Loughborough University. (n.d.). *Material Extrusion: Additive Manufacturing Research Group*. Loughborough University. Retrieved February 23, 2022, from <https://www.lboro.ac.uk/research/amrg/about/the7categoriesofadditivemanufacturing/materialextrusion/>
- [8] Loughborough University. (n.d.). *Material Jetting: Additive Manufacturing Research Group*. Loughborough University. Retrieved February 23, 2022, from <https://www.lboro.ac.uk/research/amrg/about/the7categoriesofadditivemanufacturing/materialjetting/>
- [9] Loughborough University. (n.d.). *Powder Bed Fusion: Additive Manufacturing Research Group*. Loughborough University. Retrieved February 23, 2022, from <https://www.lboro.ac.uk/research/amrg/about/the7categoriesofadditivemanufacturing/powderbedfusion/>

- [10] Loughborough University. (n.d.). *Sheet Lamination: Additive Manufacturing Research Group*. Loughborough University. Retrieved February 23, 2022, from <https://www.lboro.ac.uk/research/amrg/about/the7categoriesofadditivemanufacturing/sheetlamination/>
- [11] Loughborough University. (n.d.). *VAT Photopolymerisation: Additive Manufacturing Research Group*. Loughborough University. Retrieved February 23, 2022, from <https://www.lboro.ac.uk/research/amrg/about/the7categoriesofadditivemanufacturing/vatphotopolymerisation/>
- [12] Atkins. (2019). Additively manufactured mirrors for CubeSats. *SPIE Digital Library.*, 11116, 11116–1111616. <https://doi.org/10.1117/12.2528119>
- [13] Snell. (2020). An additive manufactured CubeSat mirror incorporating a novel circular lattice. *SPIE Digital Library.*, 11451. <https://doi.org/10.1117/12.2562738>
- [14] Boschetto. (2019). Selective Laser Melting of a 1U CubeSat structure. Design for Additive Manufacturing and assembly. *Acta Astronautica.*, 159, 377–384. <https://doi.org/10.1016/j.actaastro.2019.03.041>
- [15] Sanchez. (2018). 3D-Metal-Printed 60 GHz Offset Dual-Reflector Antenna with Integrated Conical Feed Horn and Circular-to-Rectangular Waveguide Transition. In *12th European Conference on Antennas and Propagation (EuCAP 2018): 9-13 April 2018, London, UK* / (pp. 5–5). Institution of Engineering and Technology.
- [16] Stevenson. (2020). Design and optimization of a multifunctional 3D-Printed structure for an inspector Cubesat. *Acta Astronautica.*, 170, 331–341. <https://doi.org/10.1016/j.actaastro.2020.01.012>
- [17] Li, Z.-hua, Nie, Y.-fei, Liu, B., Kuai, Z.-zhou, Zhao, M., & Liu, F. (2020). Mechanical properties of alsi10mg lattice structures fabricated by selective laser melting. *Materials & Design*, 192, 108709. <https://doi.org/10.1016/j.matdes.2020.108709>
- [18] “6U CubeSat Design Specification Rev. PROVISIONAL,” NASA, April 2016.
- [19] Wang, S., Schenk, M., Jiang, S., and Viquerat, A., “Blossoming Analysis of Composite Deployable Booms,” *Thin-Walled Structures*, Vol 157, 2020. <https://doi.org/10.1016/j.tws.2020.107098>.
- [20] Liu, S., Theoharis P., Raad R., Tubbal F., Theoharis A., Iranmanesh S., Abulgasem S.,

- Khan M., and Matekovits L., “A Survey on CubeSat Missions and Their Antenna Designs,” *Electronics*, Vol. 11, 2022. <https://doi.org/10.3390/electronics11132021>
- [21] Knap, V., Vestergaard, L., and Stroe, D., “A Review of Battery Technology in CubeSats and Small Satellite Solutions”, *Energies*, Vol. 13, 2020. <https://doi.org/10.3390/en13164097>
- [22] Falcon 9 User Manual “Falcon User’s Manual,” SpaceX, September 2021.
- [23] Hall, N., “Rocket Thrust Summary,” <https://www.grc.nasa.gov/www/k-12/airplane/rktthsum.html>
- [24] Hall, N., “Rocket Thrust Equations,” *National Aeronautics and Space Administration*, 13 May 2021. <https://www.grc.nasa.gov/www/k-12/airplane/rktthsum.html>.
- [25] Yoder, D., “B4wind user's guide,” *National Aeronautics and Space Administration*, 5 May 2003. https://www.grc.nasa.gov/www/winddocs/utilities/b4wind_guide/mach.html
- [26] “Cubesat Propulsion Systems Overview,” *VACCO Industries*, 17 September 2019. <https://cubesat-propulsion.com/vacco-systems/>.
- [27] “Mars Cube One (Marco),” *Jet Propulsion Laboratory*. <https://www.jpl.nasa.gov/missions/mars-cube-one-marco>.

Appendix A

$$\frac{A_e}{A^*} = \left(\frac{\gamma+1}{2}\right)^{-\frac{\gamma+1}{2 * (\gamma-1)}} * \frac{\left(1 + \frac{\gamma-1}{2} * M_e^2\right)^{\frac{\gamma+1}{2 * (\gamma-1)}}}{M_e}$$

$$E = \frac{\gamma+1}{\gamma-1}$$

$$\frac{A_e}{A^*} = \left(\frac{\gamma+1}{2}\right)^{\frac{-E}{2}} * \frac{\left(1 + \frac{\gamma-1}{2} * M_e^2\right)^{\frac{E}{2}}}{M_e}$$

$$\left[\left(\frac{A_e}{A^*}\right) * M_e\right]^2 = \left\{ \frac{1 + \frac{\gamma-1}{2} * M_e^2}{\frac{\gamma+1}{2}} \right\}^E$$

$$\left[\left(\frac{A_e}{A^*}\right) * M_e\right]^2 = \left\{ \frac{\frac{2}{\gamma-1} + * M_e^2}{\frac{\gamma+1}{\gamma-1}} \right\}^E$$

$$\left[\left(\frac{A_e}{A^*}\right) * M_e\right]^2 = \left\{ \frac{\frac{2}{\gamma-1} + * M_e^2}{E} \right\}^E$$

$$R = \left(\frac{A_e}{A^*}\right)^2, X = M_e^2, P = \frac{2}{\gamma-1} = \frac{E-1}{E}, Q = \frac{\gamma-1}{\gamma+1} = \frac{1}{E}$$

$$P + Q = 1, E * Q = 1$$

$$R * X = (P + Q * X)^E$$

$$F(X) = (P + Q * X)^E$$

$$F'(X) = E * Q * (P + Q * X)^{E-1} = (P + Q * X)^{E-1}$$

$$F(0) = P^E$$

$$F(1) = (P + Q)^E = 1$$

$$F'(1) = (P + Q)^{E-1} = 1$$

$$F(X) = a + b * X + c * X^2$$

$$F'(X) = b + 2 * c * X$$

$$F(0) = a = P^E$$

$$F(1) = a + b + c = 1$$

$$F'(1) = b + 2 * c = 1$$

$$a = P^E, b = 1 - 2 * a, c = a$$

$$RX = a + b * X + c * X^2$$

$$RX = a + (1 - 2 * a) * X + a * X^2$$

$$X^2 + \left[\frac{1 - R - 2 * a}{a} \right] * X + 1 = 0$$

$$r = \frac{R - 1}{2 * a}$$

$$X^2 - 2 * (r + 1) * X + 1 = 0$$

$$X = (1 + r) - \sqrt{(1 + r)^2 - 1}$$

$$M_e = \sqrt{\left(1 + \frac{\left(\frac{A_e}{A^*} \right)^2 - 1}{2 * \left(\frac{2}{\gamma + 1} \right)^{\frac{\gamma + 1}{\gamma - 1}}} \right) - \sqrt{\left(1 + \frac{\left(\frac{A_e}{A^*} \right)^2 - 1}{2 * \left(\frac{2}{\gamma + 1} \right)^{\frac{\gamma + 1}{\gamma - 1}}} \right)^2 - 1}}$$